Chapter

Earthquake-Generated Landslides and Tsunamis

Jonas Eliasson

Abstract

Large earthquakes generate tsunamis, but when it also triggers a landslide, the tsunami may become enormous. Slide scars on the continental shelf of the North Atlantic Ocean show this. For estimating the tsunami, a translatory wave theory has been suggested. Slide data are used to estimate the amplitude of the displacement wave. The amplitudes are used to obtain wave heights at a reference point outside the breaker zone. Energy transmission formulas are used to find the wave height transfer coefficients from the source area to a reference point. Tsunami risk from several sources at a reference point is quantified using stochastic processes, and estimations of a hazard curve for the probability of landslide occurrence are carried out. The sensitivity of the hazard curve to uncertainties in determining the wave height from the individual sources turns can be evaluated. In two case studies, the Tohoku tsunami and earthquake in 2011 in Japan is found to be caused by a coseismic slip and a landslide in combination, and a hazard curve for a reference point south of Iceland is found for tsunamis in the North Atlantic Ocean.

Keywords: earthquake, tsunami, landslide, hazard

1. Introduction

The main difficulty in tsunami hazard assessment is to estimate the generation of wave energy at the source. In many cases, this is simply solved by running a CFD model and estimating the ocean surface amplitude at the source [1] from it. This estimate of the amplitudes involves many problems and can be very uncertain, when the measured amplitudes are small, but a better method is still to be found.

Sometimes it is better to estimate the initial wave itself, and when that is done, the energy transmission from the source to the point of impact can be quite accurately modeled in CFD models [2–4], if the shallow water wave equations are in the numerically stable domain.

Strong earthquakes cause large deformations of the surface of the earth, so tsunamis are more often than not strengthened by landslides triggered by the earthquake. Often the triggering earthquake does not contribute any significant amount of energy to the tsunami wave, and this seems to be the general case in the North Atlantic, where few dangerous tsunamis are reported.

There have also been speculations in the scientific community about the danger of tsunamis in the North Atlantic from gigantic glacial flood waves of volcanic origin, (jökulhlaups), emerging on the south coast of Iceland. In this case, there is a well-defined probability of occurrence [5] and clear geological evidence of the

volcanic events [6] but practically no historical evidence of tsunamis. For the landslide tsunamis, we introduce a translatory wave model to estimate the initial disturbance [7]. Block slide models are popular for this purpose [8]; in them the blocks must reach very high velocities to create a serious tsunami. The translatory wave model assumes that sliding blocks break up and become debris flows when the velocity is high enough.

When the wave crest of the tsunami approaches a beach, instability of the wave fronts, wave breaking, and reflection set in. There may be little reflection on a flat beach but large energy dissipation due to wave breaking.

Few authors discuss how this problem is to be handled in practical hazard assessment, and most often this is simply done by making all coasts completely reflecting. This is on the safe side in run-up estimation. But how the correct boundary conditions should be formulated in terms of reflection and energy dissipation in the various models reported is an open question.

The following treatment on tsunamis has the emphasis on the estimation of initial disturbance and energy formation in the tsunami. The underlying theories are formulated in [8, 9] and the case studies in Chapter 7. The theory of CFD modeling of a tsunami and the associated procedures of preparing tsunami warnings are left out, as they can be found in various internet resources of the government institutions that make them.

2. Properties of a tsunami wave

Tsunamis are ocean waves that are considerably different from the best known types of ocean waves, storm waves, and ocean tides. There is much less periodicity in tsunamis, and they can run over dry land in a more or less unpredictable way. On dry land, large tsunami waves have a devastating power that resembles flood waves of the type "translatory waves" [6], such waves knock down most everything in their way. Out in the oceans (deep water), it is normally like a long wave and can be modeled using the shallow water wave theory. In this, it resembles the tidal wave.

However, there are several snags in the numerical modeling of tsunamis. Ordinary storm waves create steep wave crests that break in the shore line, but tsunamis are more like a bore, or a moving hydraulic jump; **Figure 1** illustrates this difference.

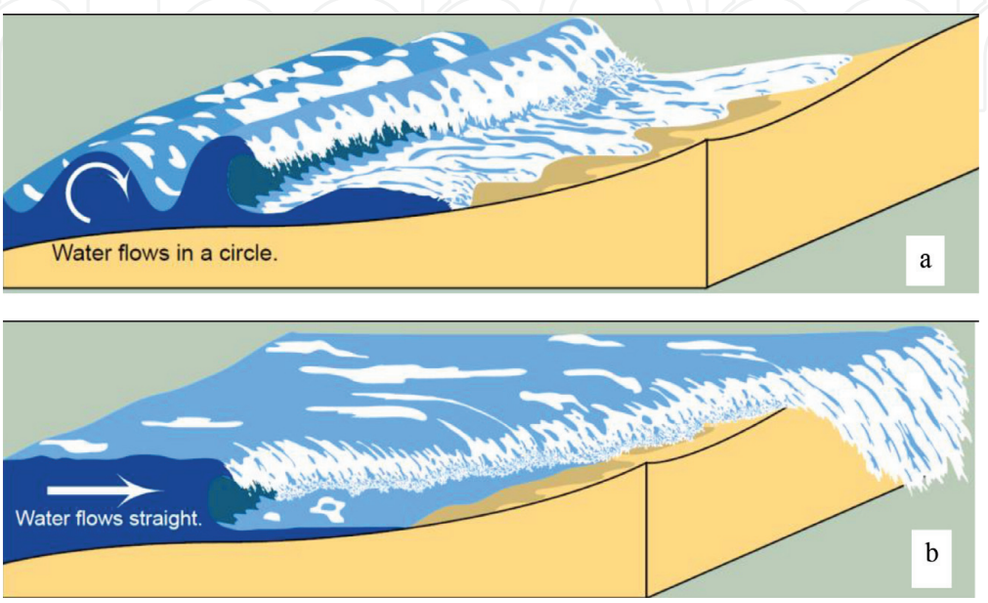

Figure 1.
Difference between storm waves (a) and tsunamis (b) [9].

Figure 2.
Nearshore breakup of a tsunami wave in Phi Phi Island 2004.

How the final inundation height is affected is unclear. Energy is lost in the jump as the bore moves inland, but with water behind has not, so it keeps moving. Then there is the role of the bathymetry; it has an influence on the dispersion and reflection of the wave fronts that is sometimes significant and sometimes not.

In short, the mathematics and numerical schemes are well developed in tsunami modeling, but there are pitfalls that can be difficult to avoid. Even models that have been through a scrutineer's process of calibration and validation can fail. Still, the initial conditions in the source area are the biggest uncertainty. It has therefore been concluded that verification and validation are necessary for each case, even for models that have been through this process before [10].

There are several numerical methods available to treat such waves using, for example, the well-known St. Venant's equations, see [11], to take an example. But the names used here, St. Venant's equations and translatory waves, are usually not mentioned. Analytical solutions are possible for stationary flows using a wave progressing with constant velocity down an inclined plane, or in a funnel, as the translatory wave in [7]. In there it is also demonstrated that numerical solutions of the St. Venant's equations can produce exactly this kind of flow without presuming a constant velocity wave.

However, when a wave runs upwards a mild slope with constant celerity c, as a translatory wave, c will inevitably reach the shallow water wave celerity, $c = \sqrt{gD}$ (g acceleration of gravity and D the water depth) somewhere, and then the surface profile may become unstable, which can result in a breaking wave (bore) or a series of braking waves if the wave is very long. **Figure 2** shows a nearshore breakup of this kind. The successive waves, resulting from the breakup, ride upon each other making the ultimate tsunami run-up very difficult to predict, even when the deep-water wave is well known. This difficulty is discussed further in Sections 5 and 7.

3. Propagation of tsunami waves

3.1 Deep water

It sounds like a misconception, but in deep waters outside the continental shelfs, tsunamis propagate as shallow water waves. The mathematics of shallow water

waves has been investigated by many; the analytical description is well known from [12] and similar works. The equations are a system of partial differential equations of the hyperbolic type, and the solution propagates along the characteristics.

Tsunamis originate in a source area, unlike the tidal wave that propagates in the same manner in deep water but originates from a gravity potential created by the moon and the sun (astronomical tide). In a point, well away from the source area, a tsunami wave front propagates along the line drawn from the source area through the point with the phase velocity $c = \sqrt{gD}$, called the wave orthogonal. The actual water velocity is much lower than c. How much lower depends on the wave amplitude H in the point and the usual shallow water formulae for local energy, $E = \frac{1}{8}\rho g H^2$, and transported energy, $E_{tr} = E\,c$, applied for a wave train, if there is one.

The full set of the partial differential equation system for tsunami propagation is nonlinear and includes terms for Coriolis forces and shear stress at the bottom and wind stress at the surface of the ocean. However out on deep water, the shear stress terms are not dominating so the equation system is only weakly nonlinear. This means that the nonlinear interaction with the local astronomical tide will be small, so its amplitude and velocity can be added without damaging errors, while the wave stays in deep water. This is not the case in shallow water.

The wave celerity c of a tsunami is the velocity of propagation of both the surface disturbance and the transported energy. This velocity is very high when the water depth is counted in kilometers, comparable to the travel speed of a passenger jet. This has a great impact on the danger of the tsunami. The tsunami attack comes swiftly, few hours after the onset of the wave from the source area.

Prediction of tsunamis is very important in disaster prevention, and a large warning system is maintained all over the world, see, for example, https://www.tsunami.gov/. A simulation model that solves the partial differential system numerically is the heart of every warning system. The model usually simulates the real wave quite well in deep water, so the estimate for the arriving time of the attacking wave may be quite accurate even when the amplitude of it is less accurately predicted. Waves that originate from the continental shelf and run over deep water regions to their place of attack are a special problem. They usually start out as displacement waves, i.e., waves without characteristic periodicity, but change to an oscillatory wave train in deep water, and the periodicity of the wave train may be difficult to model.

Numerical simulations of tsunami waves are an invaluable part of the tsunami warning system, but the uncertainty about initial wave heights and total wave energy generation is a problem.

3.2 Shallow water

Shortly after the tsunami wave hits the continental shelf, it reaches shallow water where the processes of wave refraction and diffraction take over the propagation. The wave becomes highly nonlinear as these processes, called the shoaling, set in. The wave fronts turn toward the coast, so the angle of attack is different from the deep-water direction. An example of wave fronts curved by shoaling may be seen in **Figure 2**.

When the wave hits the shoreline, the shoaling process is finished and is followed by the run-up. Approaching the coast from a reference point, the tsunami wave runs into a new near-field process of breaking and run-up of the tsunami wave and inundation of the land. In the run-up, large tsunami waves travel ashore as spilling breakers; this is a nonlinear process. The methods to predict such processes are extremely complex; depend on the incoming wave height and natural and

manmade landscape; and are very difficult to model. The run-up wave height must be estimated for each place individually. Several mathematical solutions exist for the shoaling process, both analytical and numerical from CFD. The analytical methods mostly utilize conservation of momentum or transported energy, but they are for two-dimensional waves only. Run-up heights and attenuation are very difficult to control in numerical calculation, because of difficulties in modeling the breaking of water waves, influence of obstacles on the beach, and the amount of energy dissipated in this process [13].

In finding some expressions for shoaling and run-up of two-dimensional waves, two kinds of waves will be considered: Firstly, a displacement wave, which is translatory in nature. Secondly, an oscillatory wave is considered; it has different properties than the displacement wave. When we have big tsunamis, it will be the displacement wave that hits the nearby coasts but may become an oscillatory wave farther away from the source.

3.2.1 Displacement wave

A bore, H meters high above still water level, will be formed as the water particles cannot overtake the wave front. A bore that inundates the land travels ashore as a breaking wave. Bore is formed when the water velocity u = c. According to first-order wave theory, this leads to H = D (D is the breaking depth of the wave), but from higher-order theories and practical experience, H = 0.7 D is closer to the true value for long waves breaking on a beach. If the beach slope is only slight (e.g., river estuaries), traditional long wave mild slope equations in [13] are valid. We will have an inundation, or run-up, to a level of R = H above still water level. If the slope is steep, full or partial reflection sets in, but for steep and mild slopes, R will not exceed:

$$R = H + \frac{u^2}{2g} = H + \frac{H^2\left(\sqrt{g(H/0.7}\right)^2}{(H/0.7)^2 2g} = 1.35H \tag{1}$$

3.2.2 Oscillatory wave

The shoaling process is assumed to be near linear for tsunami waves of a very small steepness. Linear theory for shoaling means keeping the energy flux constant until the point of breaking. Then we find:

$$\frac{H_b(r)}{H} = a = \left(\frac{0.7D}{H}\right)^{1/5} \tag{2}$$

The amplification factor due to shoaling of the radial wave is denoted as a. $H_b(r)$ is the breaker height of the incoming radial wave. For waves of around 1 m coming in from the deep regions of the ocean, it can become a = 2–5. For waves of a few centimeters, it can become a = 5–10. When $H_b(r)$ is found, the run-up will be the same as in the case of the displacement wave, 1.0–1.35 times the breaking wave height.

This investigation shows that the run-up process depends very heavily on the far field wave height. But if a reference point is selected in water that is deep enough to exclude the effect of breaking on the wave height estimation, then we will have a quasi-linear transfer process from the source area to the reference point. This means that a fixed coefficient, independent of source area wave height, can be used as a

wave height transfer coefficient from the source area to the reference point. This method is utilized in Chapter 6.

4. Causes of tsunamis

Large earthquakes usually start a tsunami. The earthquake deforms the bottom landscape and creates a surface disturbance in the source area and the associated transfer of energy to the water mass. This energy is transmitted from the source area by the tsunami wave.

An earthquake of magnitude 7 or larger on the Richter scale usually starts a tsunami. However, this is a rule of thumb only; smaller earthquakes can trigger a tsunami by starting a submarine landslide on bottom slopes. If it does, the magnitude of the tsunami depends on the size of the landslide, so the tsunami can be enormous even though the earthquake is small. Some years ago, it was discovered that huge submarine landslides on the continental shelf of the North Atlantic Ocean have caused large tsunamis. In Table 7.1 in [14], 11 submarine landslides with slide volumes 20–20,000 km^3 are listed. Submarine landslides of that magnitude run as translatory waves. The deadliest tsunami attacks in the recent years have struck Indonesia and the Indian Ocean coasts; the most recent one is the Anak Krakatau volcano, where a submarine landslide of type Case 1a (see Section 5.1) caused a tsunami December 22, 2018.

If a landslide is triggered or not, it can be stated that a movement on the sea bottom creates a surface disturbance with a certain potential energy, deduced by the common methods of wave mechanics. Some kinetic energy will also be created in the boundary layer around the moving object; this is mechanical energy and can thus be converted in wave energy in the tsunami wave. But as a rule, the kinetic energy will be converted to turbulent energy that cannot be converted into wave energy and is dissipated. Thus, the total potential energy of a mass that flows from land and into the sea is not converted into wave energy; only the potential energy of the initial disturbance it causes on the sea surface contributes to the tsunami.

5. Initial disturbance and the tsunami wave energy

In estimating the mechanical wave energy generated in the source area of a tsunami, three types must be considered and separate estimates devised for each one. The different types are landslides down mountain slopes and in the water where $V > c$ (Case 1). Totally submerged submarine landslides where $V < c$ at least in for a part of the slide (Case 2) and bottom landscape features are moving vertically and horizontally (Case 3). The initial tsunami wave height is estimated. The energy transmitted to the water by the movement of the landslide is estimated from the moving mass. The total wave energy is estimated as the potential energy in the water mass the slide displaces from the still water surface, using the assumption that turbulent energy transmitted to the water cannot be regenerated as mechanical energy in the tsunami wave.

The wave energy transmission away from the source area can be translatory or by a solitary group of oscillatory waves. The wave transmission can be estimated in numerical models, and the shoaling also until either the point of breaking or where the numerical stability is lost in the model. In the following we will therefore estimate the wave energy generation in the source area and the corresponding wave amplitudes. In the following, the expressions for the wave energy and amplitude h depend on the variables listed here.

B: The width of the submarine landslide	V: Velocity of the front
y_0: The frontal height of the landslide	L_h: The length under water
x_v: Distance from the shoreline to c = V	x_w: Distance to slide front
C_m: Average wave celerity in $x_w - x_v$	$L_{hb} = L_s + (x_w - x_v)C_m/V$
L_s: Effective length of a submerged slide	ρ: Density of water

For further discussion and estimation of slide dimensions, see Section 7 and [6, 9, 15].

5.1 Case 1

In this case the surface disturbance, or the water wave, cannot run away from the translatory wave, i.e., the submarine landslide that causes it because $c < V$. The water volume above the still water level will therefore simply be equal to the displacing volume, of the submerged part of the slide. The estimates for the energy of the initial wave are for the two sub-cases: Case 1a, a slide that originates from land, and Case 1b, a slide that originates at the sea bottom.

5.1.1 Case 1a

The displaced water volume will be equal to the total submerged volume of the slide. The slide will hit the water with a great splash and run on the bottom until it stops. The water will be lifted the distance y_0 from the bottom, and this will be the resulting height of the water wave when the slide suddenly stops. In that situation, the energy added to the water will be.

$$E_{W1a} = ½y_0\rho\, g y_0 B\, L_h = ½\rho g y_0^2 B\, L_h \tag{3}$$

The wave progresses in the x direction with the shallow water velocity c. In a numerical model, the initial condition for the tsunami wave height h will be zero everywhere, except in the source area where $h = y_0$ in an area of size $B\, L_h$.

5.1.2 Case 1b

Now the slide will leave a scar, or a hole L_s long, in the seabed of volume $L_s B\, y_0$. An equal part of the slide will be outside the scar and leave a heap at the slide front. The hole and the heap have the same volume. We will find.

$$E_{W1b} = ½\, y_0\rho g\, L_s B\, y_0^{\,2} = \rho g y_0^2 B\, L_s \tag{4}$$

In a numerical model, the initial condition for the tsunami wave height h will be zero everywhere, except in the source area where $h = -y_0$ in the hole area of size $B\, L_s$ and $h = +y_0$ in the heap area.

5.2 Case 2

In this case, the slide passes the point where V = c, or the depth $D = V^2/g$, and the water wave will run away from the front of the translatory slide wave. When the slide front stops, the water wave front will be at a distance $L_{ha} = x_v + (x_w - x_v)C_m/V$

away from the shoreline. In estimating the energy, we still have to distinguish between the two schemes (a) and (b) as before.

5.2.1 Case 2a

In a point x_v from the shoreline, we have c = V, the velocity of the slide, but the slide stops at the position x_w from the shoreline. With C_m denoting the average shallow water wave velocity in $x_w - x_v$, we will have $L_{ha} = x_v + (x_w - x_v)C_m/V$ for the distance from the shoreline to the water wave front. Now we have a wave height slightly less than before.

$$h_{2a} = y_0 x_w / L_{ha} \tag{5}$$

The energy of the water wave becomes

$$E_{W2a} = \tfrac{1}{2}\, h_{2a}^2 \rho\, gB\, L_{ha} \tag{6}$$

In a numerical model, the initial condition for the tsunami wave height h will be zero everywhere, except in the source area; we will have $h = h_{2a}$ in a square of size $B\, L_{ha}$.

5.2.2 Case 2b

Assuming the slide will start where c < V, we now have $L_{hb} = L_s + (x_w - x_v)\, C_m/V$. The slide will leave a scar in the seabed of size L_sB. A part of the slide, $\kappa\, L_s (\kappa < 1)$ long, will be outside the scar and leave a hole in the scar of area of volume $\kappa y_0 L_s B$. At = 0 there will be a through in the water table approximately corresponding to this volume, but in the front of the slide, we have an initial wave L_{hb} long and h_{2b} high with the same volume as the through. Then we have.

$$E_{W2a} = \tfrac{1}{2}\left(y_0^2\, \kappa L_s + h_{2b}^2\, L_{hb}\right)\rho\, gB \tag{7}$$

In a numerical model, the initial condition for the tsunami wave height h will be zero everywhere, except in the source area; we will have a through y_0 deep and a wave h_{2b} high at time t = 0.

5.2.3 Sudden increase in depth

In both Case 1 and Case 2, the slide is very likely to be in shallow water. A sudden increase in depth is therefore possible as soon as the tsunami wave sets out from the source area. A translatory wave with the velocity V, in a place where the wave celerity is c_1, will in theory continue to flow until the bottom slope I_0 is zero, but in practice it will stop sooner. The water wave will therefore run into deeper water with higher wave velocity c_2, and that affects the wave height. When the slope where the slide is running downhill fades out to a flat bottom, there is no problem in the numerical model, but in the rare occasions when there is a sudden increase in the ocean depth just in front of that point, it may provide better results to find the height h_2 of the initial wave in the deeper water:

$$h_2 = h_1 (c_1/c_2)^{1/2} = h_1 (D_1/D_2)^{1/4} \tag{8}$$

Here index 1 refers to the shallower source area and 2 to deeper water. The energy flow Eq. (8) assumes the translatory wave motion to be preserved. The

translatory wave may be transformed into a group of oscillatory waves; the details of that wave group are unclear.

Similarly, it is not quite clear what will happen in the case when the slide starts at a depth where $c > V$. In this case, the distance x_v is not defined, but if the run time of the slide can be estimated, the water wave height can easily be found.

5.3 Case 3

A movement of the ocean bottom by an earthquake usually happens fast. The movement will leave an uplift of the ocean surface where the bottom is lifted and a sink where the bottom sinks down. Both the lift and the sink contribute to the potential energy of the disturbance.

There are two possibilities to model this: Firstly, to find the Fourier transform of the surface disturbance and, secondly, to use linear wave theory to radiate it away from the source. Analytic models can be used for this if the boundary configuration can be coped with. Otherwise, a numerical model with an initial surface disturbance of the same configuration as the bottom disturbance is the only chance.

6. Studies of individual tsunamis and regional risk assessment

6.1 Tohoku tsunami in Japan

The earthquake event and the devastation caused by this tsunami is very well documented; it is the most famous tsunami event of recent years. It took place off the Pacific coast of Tohoku, Japan, on Friday, March 11, 2011 at 05:46 UTC. It was caused by a M_w 9.0 (magnitude moment) undersea megathrust earthquake with the epicenter approximately 70 km east of the Oshika Peninsula of Tohoku with the hypocenter in approximately 30 km deep water (see **Figure 3** gray arrow).

From the data obtained in the exploratory drilling at the site shown in **Figure 3**, it was concluded in [16] that the tsunami was caused by the mass movement shown in **Figure 4**.

The details of the bottom deformation are estimated and pictured in **Figure 3b** in [18]. This picture resembles a 150 km long slide scar with L_s and B about 110 km and y_0 about 8 m using the symbols in Chapter 5.2. This would be a Case 2b slide, stopping 25–75 km from the trench, see **Figure 4**; here the average bottom slope is about 4/50 or 8–9%. It is interesting to note that layers of fine sediments on such a slope can easily liquify, slide down the slope, and cause a bottom deformation like the one pictured in [18] and indicated by black arrows in **Figure 4**. No evidence has been found in [16] to support this suggested slide event, but the information on the bottom deformation given in [18] is considered reliable, and it is supported by a coseismic slip model in **Figure 4** in [17]. The suggested slide would have characteristics that can be calculated using the equations for the Case 2b slide. If the slide is due to liquefaction, the movement will start at the onset of the strong motion and stop when it stops. According to graphs in [18], this time is about 30 seconds; this is an information additional to what we have in Sections 5.2.2 and 5.2.3.

$V = 2$ m/s corresponds to the 9% slope and $y_0 = 8$ m. Together with the time 30 s, this gives a horizontal flow path of 60 m. This corresponds well to **Figure 4**, giving 56 m as maximum horizontal deformation.

The water depth gives $c = 250$ m/s so we get $L_{bh} = 250 \times 30 = 7500$ m = 7.5 km for the initial disturbance. As the flow path is short the $\kappa \sim 0$. Now we get.

$L_{bh} = L_s + 7.5 = 110 + 7.5 = 117.5$ km.

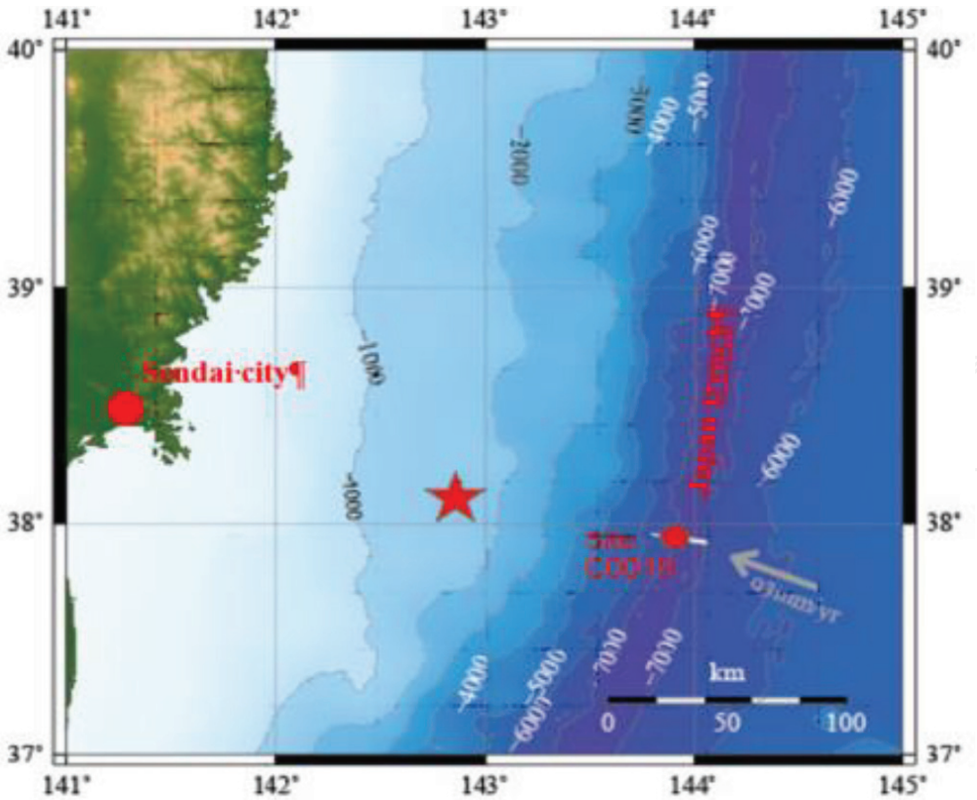

Figure 3.
Location chart of the tsunami site with the epicenter (red star) and an exploration well, drilled at site Coo 19, [16].

The uplift caused by the coseismic movement means that there will be just a small hole in the scar area. The volume of the heap caused by the slide will be.

$W_{T2b} = By_0L_s = 1 \times 110000 \times 8 \times 110000 = 9.68 \times 10^{10}$ m^3 = 96.8 km^3.

The height of the wave with same volume as in Section 5.2:

$h_{2b} = W_{T2b}/(L_{hb}\ B) = 8 \times 110/117.5 = 7.5$ m.

Eq. (7) must be modified due to the uplift and the small scar hole; this is done by putting $\kappa \sim 0$ as before, and then we have for the energy in the source area:

$E_{W2a} = ½h_{2b}^2\ L_{hb}\rho\ g\ B = ½\ 7.5^2 \times 117500 \times 1025 \times 9.81 \times 110000 = 3.6\ 10^{15}$ Nm.

This result can be checked against the simulation results published by NOAA [19]; it is on **Figure 5** and shows the spread of the tsunami very well. Comparing this with a ring wave spreading in an effective 90° conical channel gives a resulting average wave height 2–3 feet 900 km from the source. According to C = 250 m/s (800 km/h), this should occur after little more than 1 hour. This checks well against **Figure 5**.

The bottom deformations that caused the very strong Tohoku tsunami in the Pacific Ocean, simulated numerically by the Japanese and USA scientists, [17, 19], can be explained by a submarine landslide. This suggests that the coseismic slip of the earthquake triggers a sliding of the surface sediments. In combination they cause the bottom deformation. Finally, it can thus be concluded that the coseismic slip and the landslide are both responsible for the Tohoku tsunami in March 2011, not the coseismic slip alone.

This shows that in assessing the tsunami risk in the Pacific coastal regions of Japan, the landslide risk must be considered. This fact may result in that considerably larger events than the Tohoku tsunami are possible if a larger slide than this 8 m thick slide is released. This landslide is not very high compared to what has happened elsewhere. The assessment of this possibility of larger slides can be

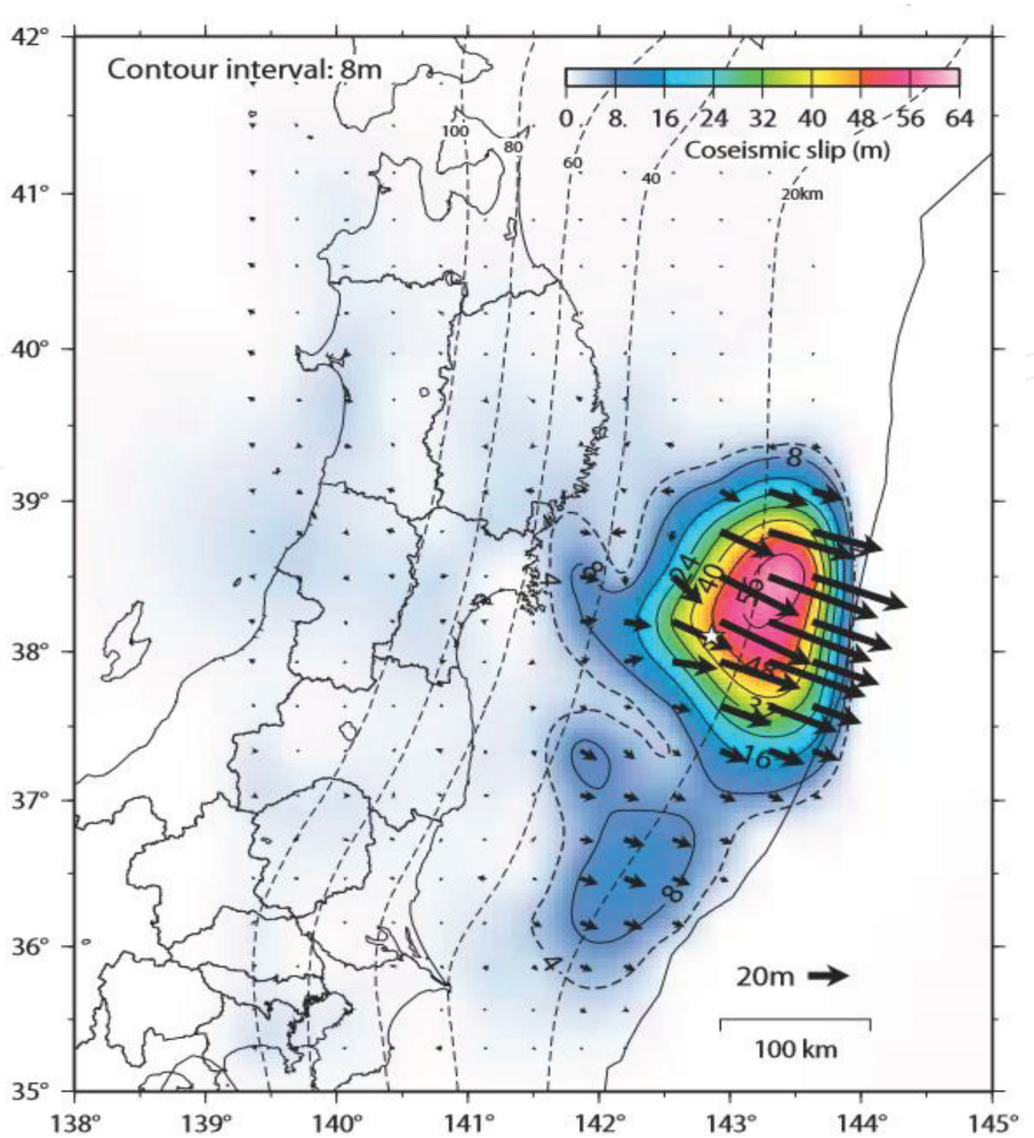

Figure 4.
The 2011 Tohoku earthquake: Coseismic slip distribution model, from [17].

difficult; there is considerable uncertainty in estimating the height (y_0) of possible landslides.

6.2 Tsunami risks in the North Atlantic Ocean

There are many tsunami sources in the Atlantic Ocean, but in the northern regions, the tsunami risk is less than in many other places, and the source of the main threat may be unknown, both location and magnitude. A good method is presented in [9], to estimate the hazard curves for a reference point in south Iceland. This involves estimating initial wave heights at the source and their frequencies. Then the transfer functions must be applied, and the hazard curves are found by numerical integration.

6.2.1 Risk assessment methods

To assess the risk, we have to estimate event return periods for the various event magnitudes and the correlation structure of the event history. This correlation may be between time length between events and event magnitude and autocorrelation (positive or negative) in the time history.

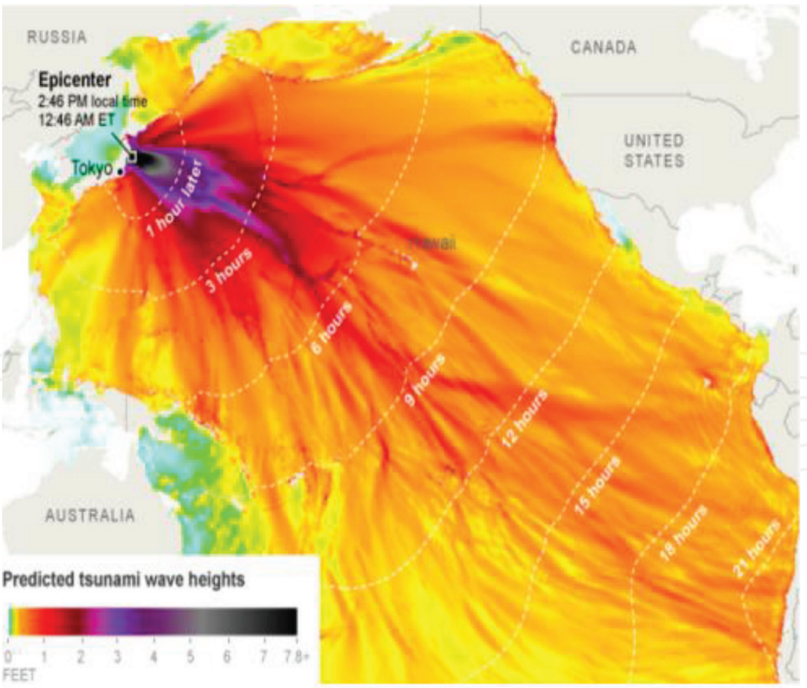

Figure 5.
Spreading of the Tohoku tsunami in the Pacific Ocean March 11, 2011. (NOAA Center for tsunami research, Pacific marine environmental laboratory; NOAA. 2011. Printed in the N.Y. Times).

The very long records necessary for a complete picture of the event statistics are normally not available. Certain assumptions are necessary, but we must estimate the basic statistics such as average time between events, t_a, the standard deviation associated to it, t_s and the correlation between magnitude and event interval ρ (note the different meaning of ρ in chapter 5). Now the following formula can be derived for the interval between tectonic events, it being earthquakes, submarine slides, or volcanic events:

$$g_k(i) = \rho\, h_k(i) + \sqrt{(1-\rho^2)}\, e_k(i) \tag{9}$$

i	Number of event occurring at time t(i)
$g_k(i) = ((t(i+1) - t(i) - t_a)/t_s$	Dimensionless relative time between events
$h_k(i) = \rho(H_k(i) - H_a)/H_s$	Relative magnitude, e.g., wave height
$\rho = E\{g_k(i)h_k(i)\}$	Magnitude time correlation (E denotes average)
$e_k(i)$	Random function $e_k(0.1)$
k	Series number

The time between the tectonic events i and i + 1 is known when $g_k(i)$ is known so series for the occurrence of events in time can be simulated when $h_k(i)$ is known. If the simulation period is a limited number of years into the future, it is necessary to simulate sufficiently many series (the number k) so the statistical distribution of H is represented.

If this statistical distribution is not known, some classification that fits available observations of H has to be assumed. Three classes, small, medium, and large events, should be considered as minimum. Then the Monte Carlo method is used to simulate the k series, and they are used to determine the statistics of interest

empirically. These are various hazard curves and event probabilities for fixed periods to come, e.g., economical lifetime of structures and so on. It must be noted that the probability of a specified event of a given class happening in the next year is not a constant. This probability will increase with time.

6.2.2 Example from South Iceland

There are several methods to estimate the distribution functions we have to use as building blocks in Eq. (9) recommended in the literature. The log-normal distribution is often usable for g_k, especially when ρ is low [5].

When there is more than one source, the procedure has to be repeated for all significant sources. Then the transfer functions have to be applied and H_a and H_s calculated for the chosen reference point. H_s is much more difficult to estimate from observations than H_a, but sometimes it is possible to estimate the coefficient of variation $C^v = H_a/H_s$. If not it has to be included as a parameter in order to estimate the accuracy of calculated probabilities and risks.

In [9], all this is done for a reference point south of Iceland. There are eight possible sources for tsunamis in the North Atlantic, six of these are found significant for the reference point chosen. For clarification the reference point is shown and the resulting risk curve.

The only significant Icelandic source contributing to the calculated tsunami height in the reference point on **Figure 6** is the Katla volcano [6]. The hazard curves for these points are in **Figure 7**. Here all the risk curves follow the Gumbel distribution $P(H > x) = \exp(-\exp(-y))$ where $y = 3.91 + 1.12\,x$ rather closely. Here the probability P does not denote the next event, but the maximum to be expected in the next year (annual maximum); it will be $x = (y - 3.91)/1.11$ in each point in **Figure 7**.

Figure 6.
Icelandic coastal waters, depth scale by deeper blue for each 200 m. Population centers in red [9].

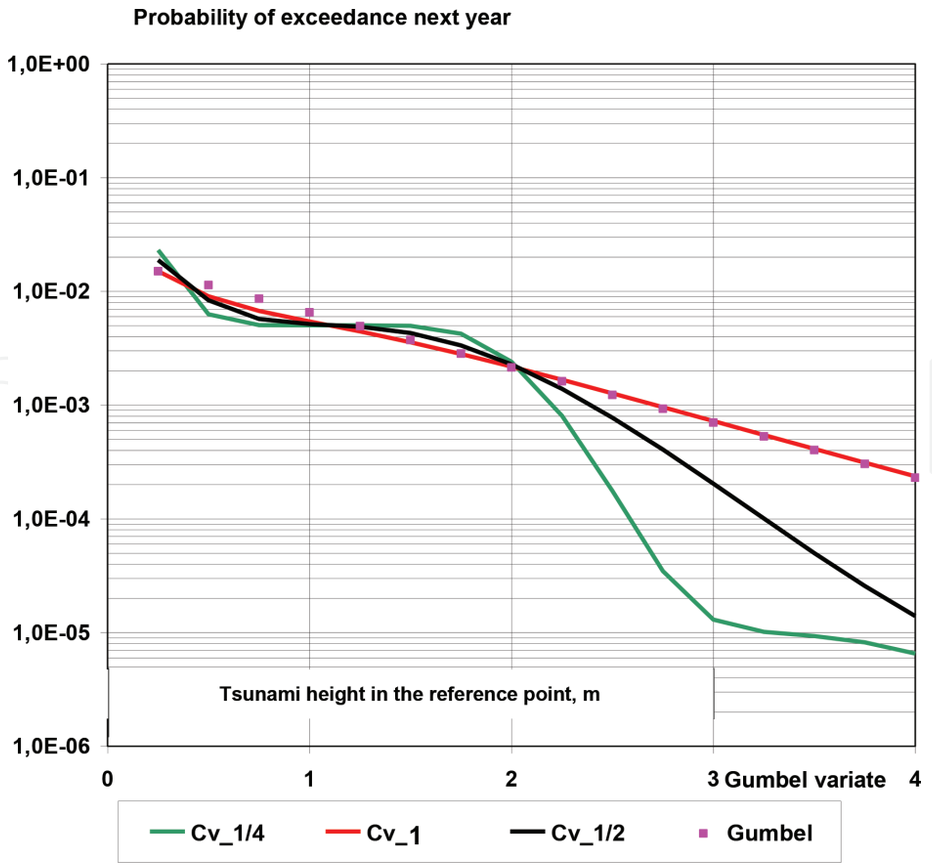

Figure 7.
Hazard curves for the reference point with three different C^v values. The abscissa is the Gumbel variate [9].

The probability is for the maximum to be expected in the next year (annual maximum). To take an example, the maximum to be expected in the very next year with probability P = 1% or 0.01 has the Gumbel variate 0.4, corresponding to a wave height of x = 0.1 m which is rather insignificant, but for P = 0.1%, the Gumbel variate is 2.8 giving seven times larger wave height.

7. Discussions

Tsunami attack is very difficult to predict, even though the models that simulate the propagation of the tsunami wave over deep water are very good and in most cases reliable. The mathematics of these models is very difficult, but effective, as long as the wave stays in deep water [20]. The difficulty in modeling is to predict the shoaling and the run-up. And then there is the uncertainty about the initial wave height and wave energy formation in the source area.

The importance in such analysis is to identify the sources that cause the largest tsunami threats. The methods devised in Chapter 5 can be used to estimate the initial wave and energy in the source area when the bottom deformation is known. This is demonstrated in the case study of the Tohoku tsunami, in Section 6.1; in [21] is a detailed description of this huge event and its consequences.

The cause of the bottom deformation is directly or indirectly an earthquake. It can start a submarine landslide, or the earthquake wave itself can deform the bottom so much that a large tsunami is produced, especially earthquakes above 7 in magnitude. But this very information tells us that the variability in tsunami properties will be very great in the source area. The magnitude of the average event may be possible to estimate from existing observations and geophysical data, but their

standard deviation will always be difficult to estimate; usually there are not enough observations of serious tsunami events to establish a reliable value for this coefficient.

In the example taken in Section 6.2, there are eight identified tsunami sources in the North Atlantic Ocean, six of these contribute significantly to the hazard curve in the danger zone on **Figure 7**. This is the zone above 2 m, meaning that the tsunami has to be 2 m or higher to pose any significant threat alone, i.e., without being accompanied by a flood of different origin [9] or attacking upon a spring tide flood.

The effect of the coefficient of variation on the hazard curve **Figure 7** is quiet surprising. The estimation of its value is very difficult. However, to leave it out corresponds to estimating its value to be zero, and that is totally unsatisfactory. In **Figure 7** the effect of three different values, common in geophysical data, is demonstrated, and the difference is quite striking. The difference in frequency of occurrence is of one decade, up or down, from the $C^v = 1/2$ value.

8. Conclusion

The translatory wave theory is used to estimate the expressions for energy and wave height in the source area, and it can be used for the initial conditions in wave models.

Earthquakes, of too small a magnitude to produce dangerous tsunamis themselves, can do so by triggering submarine landslides.

Approximate analytical methods can give good results as a first approximation for the transfer functions that link the wave heights in the source area to wave heights in a reference point selected in the wave propagation path. The best position for such a point is offshore, outside the zone of nonlinear shoaling and wave breaking, but near the places where the attack of the tsunami is expected. Then a hazard assessment may produce a wave height-frequency curve for this point.

It is clearly demonstrated that it is very important to include the C^v factor for the event magnitude in the hazard assessment. Otherwise the tsunami wave heights for a given frequency may be seriously underestimated.

For high C^v values the hazard curves may be expected to follow the Gumbel distribution or possibly another distribution of the extreme value distribution family because the hazard curve is the maximum expected frequency for a given wave height.

Acknowledgements

Part of the theories herein is developed for the Básendaflóð (The Flood at Basendar Iceland in 1799) research directed by Sigurður Sigurðarson, Section Engineer, Icelandic Road and Coastal Administration, and in cooperation with Gísli Viggósson Consulting Engineer, Reykjavík Iceland. This project was supported financially by the Research Fund of the Icelandic Road and Coastal Administration who also sponsored this publication. Their support is greatly acknowledged.

The authors acknowledge Japan Agency for Marine-Earth Science and Technology and the NOAA Center for Tsunami Research, Pacific Marine Environmental Laboratory, for the use of material referred by them.

Conflict of interest

The author declares that there are no conflict of interests regarding the publication of this chapter.

Author details

Jonas Eliasson
Earthquake Engineering Research Centre, School of Engineering and Natural Sciences, University of Iceland, Iceland

*Address all correspondence to: jonaseliassonhi@gmail.com

References

[1] Benfield Hazard Research Centre. Tsunami Hazards in the Atlantic Ocean. London, England: The Centre; 2003

[2] Kerridge D. The Threat Posed by Tsunami to the UK. London, UK: Department for Environment, Food and Rural Affairs, Flood Management Division; 2005

[3] Ward SN, Asphaug E. Asteroid impact tsunami of 2880 March 16. Geophysical Journal International. 2003; **153**(3):F6-F10

[4] Tinti S, Bortolucci E, Armigliato A. Numerical simulation of the landslide-induced tsunami of 1988 on Vulcano Island, Italy. Bulletin of Volcanology. 1999;**61**(1–2):121-137

[5] Eliasson J, Larsen G, Gudmundsson MT, Sigmundsson F. Probabilistic model for eruptions and associated flood events in the Katla caldera, Iceland. Computational Geosciences. 2006; **10**(2):179-200

[6] Elíasson J. A glacial burst tsunami near Vestmannaeyjar, Iceland. Journal of Coastal Research. 2008;**241**:13-20. https://doi.org/10.2112/05-0568.1

[7] Elíasson J, Kjaran SP, Holm SL, Gudmundsson MT, Larsen G. Large hazardous floods as translatory waves. Environmental Modelling & Software. 2007;**22**(10):1392-1399

[8] Tinti S, Bortolucci E, Vannini C. A block-based theoretical model suited to gravitational sliding. Natural Hazards. 1997;**16**(1):1-28

[9] Eliasson J, Sigbjörnsson R. Assessing the risk of landslide-generated Tsunamis, using translatory wave theory. International Journal of Earthquake Engineering and Hazard Mitigation. 2013;**1**(1):61-71

[10] Synolakis CE, Bernard EN, Titov VV, Kânoğlu U, Gonzalez FI. Validation and verification of tsunami numerical models. In: Tsunami Science Four Years after the 2004 Indian Ocean Tsunami. Basel: Birkhäuser; 2008. pp. 2197-2228

[11] Julien PY. River Mechanics. New York, United States of America: Cambridge University Press; 2002

[12] Stoker JJ. Water Waves. NY: Interscience Publishers; 1957

[13] Svendsen IA. Introduction to Nearshore Hydrodynamics. Singapore: World Scientific; 2006

[14] Bryant E. Tsunami—the Underrated Hazard. 3rd ed. Springer International Publishing; 2014. DOI: 10.1007/978-3-319-06133-7

[15] Rupakhety R, Ólafsson S, editors. Earthquake Engineering and Structural Dynamics in Memory of Ragnar Sigbjörnsson: Selected Topics. Chapter 8. Springer; 2017

[16] JAMSTEC. Causal Mechanisms of Large Slip during the Tohoku Earthquake of 2011. Revealed through Hydraulic Analysis of Fault Drilling Samples from the Deep–Sea Scientific Drilling Vessel Chikyu; Japan Agency for Marine-Earth Science and Technology. 2013. Available from: http://www.jamstec.go.jp/e/about/press_release/20131008/

[17] Land and Sea Areas of Crustal Movement and Slip Distribution Model of the Tohoku-Pacific Ocean Earthquake: Coseismic Slip Distribution Model. Report by the Geographical Survey Institute, Japan. 2011. Available from: http://www.gsi.go.jp/cais/topic110520-index-e.html

[18] Fujii Y, Satake K, Sakai SI, Shinohara M, Kanazawa T. Tsunami

source of the 2011 off the Pacific coast of Tohoku earthquake. Earth, Planets and Space. 2011;**63**(7):55

[19] Available from: https://www.youtube.com/watch?v=Lo5uH1UJF4A&feature=youtu.beNOAA. 2011

[20] Dutykh D, Dias F. Energy of tsunami waves generated by bottom motion. Proceedings of the Royal Society A: Mathematical, Physical and Engineering Sciences. 2008;**465**(2103):725-744

[21] Wikipedia. 2011 Tohoku earthquake and tsunami. 2016. Available from: https://en.wikipedia.org/wiki/2011_T%C5%8Dhoku_earthquake_and_tsunami